Aging effects on the nucleation of Pb nanoparticles in silica

F. P. Luce, F. Kremer, S. Reboh, Z. E. Fabrim, D. F. Sanchez et al.

Citation: J. Appl. Phys. **109**, 014320 (2011); doi: 10.1063/1.3530844
View online: http://dx.doi.org/10.1063/1.3530844
View Table of Contents: http://jap.aip.org/resource/1/JAPIAU/v109/i1
Published by the American Institute of Physics.

Aging effects on the nucleation of Pb nanoparticles in silica

F. P. Luce,[1] F. Kremer,[1] S. Reboh,[1,2] Z. E. Fabrim,[1,2] D. F. Sanchez,[1] F. C. Zawislak,[1] and P. F. P. Fichtner[1,2,a)]
[1]*Instituto de Física, Universidade Federal do Rio Grande do Sul, Porto Alegre 91501-970, Brazil*
[2]*Escola de Engenharia, Universidade Federal do Rio Grande do Sul, Porto Alegre 91501-970, Brazil*

(Received 11 August 2010; accepted 23 November 2010; published online 13 January 2011)

The ion beam synthesis of Pb nanoparticles (NPs) in silica is studied in terms of a two step thermal annealing process consisting of a low temperature long time aging treatment followed by a high temperature short time one. The samples are investigated by Rutherford backscattering spectrometry and transmission electron microscopy. The results obtained show that highly stable Pb trapping structures are formed during the aging treatment. These structures only dissociate at high temperatures, inhibiting the nucleation of NPs in the metallic phase and causing an atomic redistribution that renders the exclusive formation of a two dimensional, uniform and dense array of Pb NPs at the silica–silicon interface. The results are discussed on the basis of classic thermodynamic concepts. © *2011 American Institute of Physics*. [doi:10.1063/1.3530844]

I. INTRODUCTION

The formation of dispersed second phase nanoparticle (NP) systems in silica films via ion beam synthesis have been extensively studied in connection with technical applications exploring luminescent[1–3] or electrostatic[4–6] (Coulomb blockade) properties for the development of silicon based devices. The primary concept behind the ion beam synthesis method relies on the formation of a supersaturated solid solution produced by the implantation process, followed by the nucleation and growth of the new phase upon post-implantation thermal treatments. The obtained system comprises a dispersion of NPs within the film according to the depth distribution of the originally ion implanted profile. Their growth follows a nonhomogeneous coarsening process which produces both size and depth dispersed NP systems.[7–10]

We have previously demonstrated that the classical nucleation route observed for most metal atoms implanted into silica films can be avoided in the case of Sn.[11] It was argued that, during a low temperature long-term thermal treatment (aging), there is formation of small atomic clusters with high thermal stability. In the present work we show that the same phenomenon observed for Sn also happens in the case of Pb. This represents a more general behavior and shows that Sn or Pb in silica are interesting model case elements for the study of embedded NP melting point depression or elevation.[12–14] The results are discussed based on particular atomic bonds and interface properties, thus tackling on a new thermal stability behavior of atomic clusters in silica.

II. EXPERIMENT

Pb^+ ions were implanted with an energy of 300 keV in order to locate them around the center of a 200 nm thick silica layer thermally grown via dry oxidation of a (001) Si substrate. The implantations were performed at room temperature to a fluence of $\phi = 5 \times 10^{15}$ cm^{-2}. After implantation, the samples were submitted to distinct thermal treatments: (i) high vacuum furnace annealing (FA) at T = 1370 K during 1 h and (ii) aging treatment in air at T = 473 K for 100 h followed by the FA treatment described above. In order to test the Pb NPs stability in silica, an additional sample was implanted to a larger fluence ($\phi = 1 \times 10^{16}$ cm^{-2}) and was FA treated for a longer period (6 h). The thermal evolution of the ion implanted profiles was characterized by Rutherford backscattering spectrometry (RBS) measurements using a 1.2 MeV He^+ beam from a 3 MV HVEE Tandetron accelerator. The microstructure of as-implanted, aged and FA samples was characterized by transmission electron microscopy (TEM) using cross-section and plan-view species prepared by ion milling. The TEM observations were carried out in a JEM 2010 microscope operated at 200 kV.

III. RESULTS

Figure 1(a) shows the Pb atoms concentration-depth profiles from the as-implanted and directly FA (1 h) treated samples. The RBS results appear superposed to a cross-section TEM micrograph from the FA (1 h) sample. It is clear that the FA treatment causes the Pb redistribution and the nucleation and growth of NPs. About 10% of Pb atoms become trapped at the silica–silicon interface, forming small NPs. Although these particles at the interface are not spherical, their size distribution can be characterized by a mean diameter d_m of ≈5.3 nm and standard deviation σ of ≈0.6 nm. A larger fraction of the Pb atoms (≈70%) is contained within the NP system ($d_m \approx 10$ nm and $\sigma \approx 3.5$ nm) and dispersed along the film, while a fraction of ≈20% is lost by evaporation. Figure 1(b) shows that, for a longer FA treatment (6 h), the release of Pb atoms from the spherical NPs within the silica film results in the formation of cavities presenting a conspicuous oblate shape, as well as the increase in the relative Pb content at the interface resulting in a total fraction of ≈20% of the implanted content.

a)Electronic mail: paulo.fichtner@ufrgs.br.

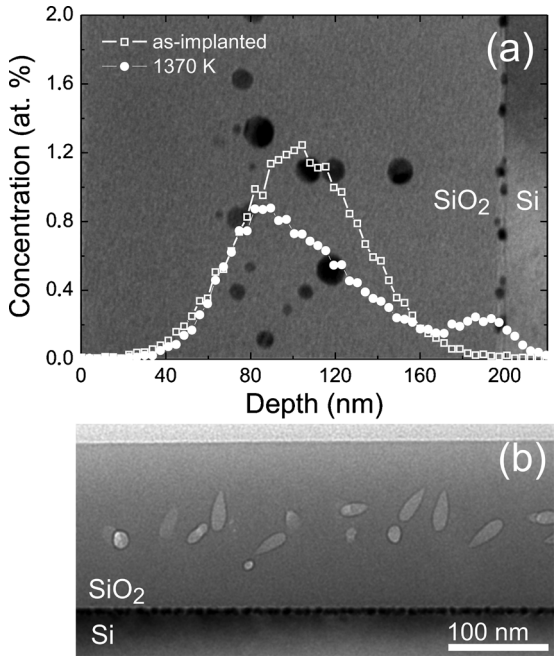

FIG. 1. (a) RBS measurement presenting the concentration-depth profile of the Pb atoms in as-implanted and FA (1 h) samples. Its background contains a cross-section TEM micrograph from the FA (1 h) sample slightly tilted from the [011] zone axis to avoid strong diffraction contrast. (b) Cross-section TEM micrograph from a FA (6 h) treated sample. Notice the formation of voids in the silica film and the NP array at the silica–silicon interface (underfocus).

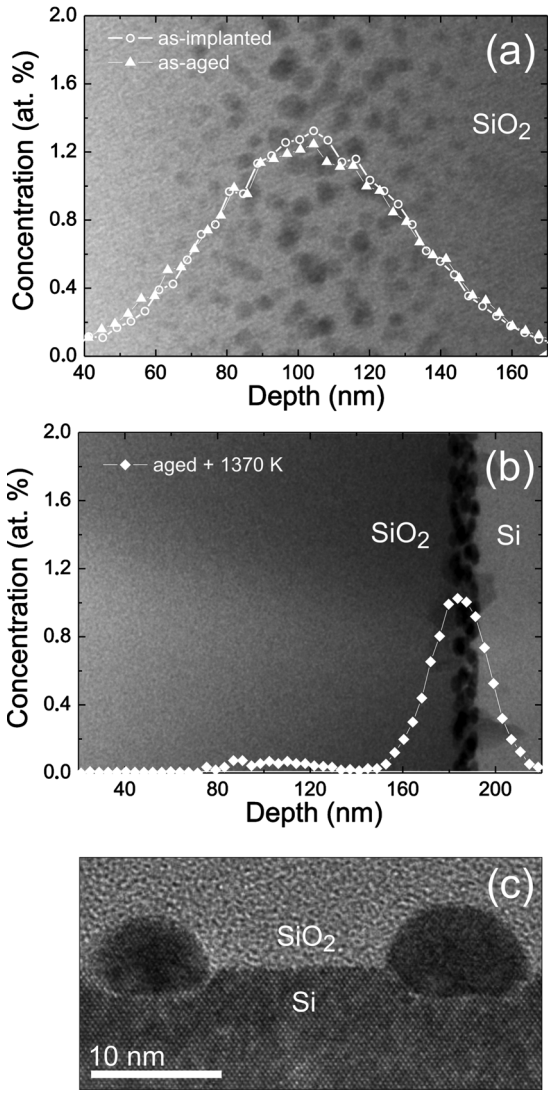

FIG. 2. (a) RBS measurement presenting the concentration-depth profile of the Pb atoms in as-implanted and as-aged samples. Its background contains a cross-section TEM micrograph from the as-aged sample (underfocus). (b) RBS measurement from an aged and subsequently FA (1 h). Its background contains a cross-section TEM micrograph taken at 8° tilted direction from the [011] zone axis, providing a perspective view of the NP arrangement at the silica–silicon interface. (c) High resolution cross-section image of the NPs at the silica–silicon interface. Their shape is characterized by a spherical dome in the silica side and a pyramidal frustum in the silicon matrix.

Figure 2 illustrates the aging treatment effect. The RBS profiles from as-implanted and aged samples are nearly identical [Fig. 2(a)]. TEM observations of the as-implanted samples do not present remarkable features. However, the as-aged samples [background of Fig. 2(a)] present a NP array characterized by $d_m \approx 4.2$ nm and $\sigma \approx 0.8$ nm distributed along the implanted profile. From tilted images presenting the projection of the silica–silicon interface, we were able to determine an upper limit of the sample thickness within a given observation area, allowing the evaluation of the NP concentration. Using their size distribution and assuming that the particles contain only Pb atoms arranged in a densely packed structure similar to the fcc bulk metallic phase, we estimate that the Pb content in these TEM visible NPs has an upper limit of ≈25% of the implanted amount. However, TEM contrast analysis presents a less intense mass or diffraction contrast, suggesting that the particles are not of the metallic fcc Pb phase and have a poor crystallinity. Therefore, we may consider that such TEM observable particles correspond to a Pb oxide structure, so that the remaining Pb content within TEM invisible clusters can be even larger than 75%. Upon subsequent FA (1 h) treatment [Fig. 2(b)], the RBS measured profile of aged samples shows that most of the Pb content redistributes, either toward the surface or the interface sinks. In addition, the small NPs observed in the as-aged samples [Fig. 2(a)] disappear resulting in no TEM observable cavities. This microstructure evolution results in the recovery of the oxide film to an apparent pristine aspect and in the formation of a dense NP array at the silica–silicon interface containing a fraction of ≈38% of the implanted fluence. More detailed TEM observations reveal that the silica film presents very few but large Pb NPs [not shown within the observation field of Fig. 2(b)], consistent with the small fraction of atoms remaining inside the silica as detected by RBS. Figure 2(c) presents an enlarged cross-section view of the NPs at the interface. They can be characterized by a spherical dome in the silica side and a pyramidal frustum in the silicon matrix. Figure 3 shows a plan-view micrograph from the interface region of an aged and FA (1 h) treated sample [Fig. 3(a)], the corresponding selected area diffraction pattern (inset) and the calculated pair correlation function of the planar NP arrangement [Fig. 3(b)]. The plan-view observations demonstrate that the NP frustums within the Si side present a square base, the NPs lattice corresponds well to the metallic phase Pb fcc structure, and that the particles are epitaxially oriented with respect to the Si lattice. Their number density is ≈3.7

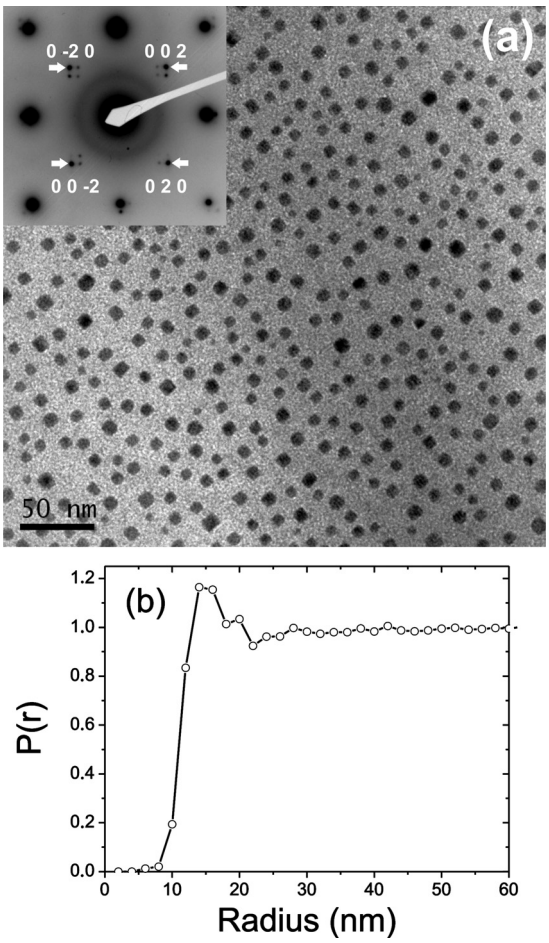

FIG. 3. (a) Plan-view TEM micrograph showing the characteristic NP arrangement along the silica–silicon interface. Notice that the edges of their square basis are aligned along the [001] directions of the Si matrix. The inset shows a selected area diffraction pattern along the [001] zone axis of the Si matrix where the strong reflections are form the Si lattice. The indexed reflections are from the (002) planes of the metallic fcc structure of the Pb particles. The weaker reflection features correspond to double diffraction effects. Notice that the Pb reflections appear symmetrically distributed around the Si ones, thus proving the epitaxial orientation of the NPs. (b) Pair correlation function $P(r)$ of the planar NP arrangement. Its peak position indicates a mean first neighbor distance D_m of ≈15 nm and a standard deviation σ_D of ≈3 nm.

$\times 10^{11}$ cm^{-2}. The size distribution obtained from plan-view micrographs is characterized by a narrow size dispersion with a mean lateral size L_m of ≈8.2 nm and a standard deviation σ_L of ≈1.17 nm. The calculated pair correlation function[15] shows a well dense near neighbor distance D_m of ≈15 nm with a dispersion σ_D of ≈3 nm, thus indicating a certain degree of near neighbor order as indicated by the shoulder of the first peak. Finally, it seems remarkable that, either for aged or non aged samples, FA treatments cause the dissolution of the observed particles or clusters within the silica film [see, Figs. 1(b) and 2(b)], but the NPs at the silica–silicon interface remain stable.

IV. DISCUSSIONS

Figure 2 summarizes the results obtained after the aging treatment. They contrast significantly with the typical ion beam synthesis behavior observed for the non aged samples (see Fig. 1), usually described by classical thermodynamic concepts discussed elsewhere.[7–10] Upon aging, two sets of structures are formed. The first set consists of TEM observable particles [Fig. 2(a)], corresponding to a fraction of less than 25% of the implanted content that can be regarded as a Pb-oxide phase. These particles do not coarsen, but only dissociate during the FA treatment. Since the FA treatment is done under high vacuum conditions, it is highly probable that their coarsening does not proceed due to the lack of oxygen supply. The second set is associated with structures trapping the majority of the Pb content (fraction larger than 75% of the implanted fluence). The presence of Pb is detected by RBS but the corresponding trapping structures cannot be observed by TEM. Considering that silica embedded clusters containing heavy atoms and with diameters larger than ≈1.2 nm are clearly distinguished by TEM, we can state that the trapping structures are smaller. This renders an upper limit of ≈30 atoms per cluster if their density corresponds to the bulk metallic Pb phase. Only upon FA (1 h) treatment at 1373 K these structures dissociate, since RBS measurements show that the Pb atoms migrate toward the surface (evaporating) or toward the silica–silicon interface. From the present results we can state that the massive Pb redistribution process observed in the aged and subsequently FA (1 h) treated samples is not related to the formation of large particles inside the silica film, otherwise cavities would be observed since SiO_2 molecules cannot refill the void left by a large NP [see Fig. 1(b)].

In the following, we will phenomenologically discuss the thermal stability of Pb agglomerates in silica, assuming that classical thermodynamic concepts may be extended to small particles. For the discussions, since the FA treatments are performed at a temperature significantly higher than the melting temperature of the bulk Pb metallic phase, we will consider the liquid Pb phase as a fiducial state which prevails during the FA treatments of non aged samples. Hence, the coarsening evolution taking place for the non aged samples can be described by the Gibbs–Thomson (GT) relation

$$C(r) = C_o \exp(2\gamma\Omega/rk_bT).$$

This equation represents the solute field of Pb atoms around a particle of radius r, where C_o is the thermal equilibrium solubility, γ the interface energy, Ω the Pb atomic volume, k_b the Boltzmann constant and T the temperature. According to the GT relation, particles with large r and/or small γ tend to become more stable since their local equilibrium condition is readily achieved by the dissociation of a small number of atoms. Hence, when liquid Pb particles are formed, the results obtained suggest that their interface energy γ is sufficiently high to cause the dissolution of the smaller particles that sustain the growth of the larger ones. As the coarsening proceeds, the decrease in their number density to a level where the mean distance between particles is of the order of their distance to the surface or to the interface sinks, the diffusional interactions with the sinks cause the loss of Pb content from the NP system, thus resulting on the formation of voids [Fig. 1(b)]. Opposed to this situation, we assume that the aged samples cannot present liquid particles, otherwise they would be converted into the fiducial phase and reproduce the results of the non aged case. Hence, upon ag-

ing, the Pb atoms can only be trapped within small structures (invisible by TEM) which remain solid and only dissociate at high temperatures, thus inhibiting the formation of liquid Pb particles since their nucleation probability decreases with the increase in temperature. There are two plausible possibilities to fulfill these conditions. First, the formation of oxide structures such as lead oxide[16] or lead tetroxide,[17] which present bulk melting temperatures of 1161 K and 773 K, respectively. Such particles may become stable even for small sizes according to the interface arguments discussed below. Second, the formation of Pb clusters such as the predicted by density functional theory calculations for free standing structures.[18,19] These clusters are characterized by a small number of atoms (32 or less), and their high thermal stability is a result of the increase in their cohesive energy due to the formation of stiffer covalent bonds and the formation of specific topological arrangements that avoid dangling bonds.[18–20] Our results comprise silica embedded clusters which necessarily require the formation of atomic bonds with the surrounding matrix and, therefore, may not reproduce the same structures proposed for the free standing cases. However, the formation of similar covalent bonded clusters presenting fully coherent interfaces (i.e., without dangling bonds) with the silica matrix can result into a system with very low interface energy. On the basis of thermodynamic models,[13,21] the melting temperature T_m of NPs varies with respect to the corresponding bulk value T_b as a function of their radius r as

$$\frac{T_m}{T_b} = 1 + \frac{k(\gamma_l - \gamma_s)}{r}.$$

In this equation γ_l and γ_s are the interface energies of the liquid and solid particles and k is a constant depending on the latent heat of melting and on the atomic density of the particles. In the present case, we may assume that γ_s from the particles is smaller than γ_l from the fiducial liquid state. Under such conditions, the decrease in T_m usually observed for metallic NPs can be reversed, resulting in the increase in their thermal stability and, therefore, providing a consistent explanation for the present experimental data. Our results for Pb are also consistent with the previous ones for Sn.[11] Hence, we may conclude that these experimental findings comprise a more general behavior, so far observed for elements as Sn and Pb that either form covalently bonded clusters or oxide phases with high melting temperatures. Additional experiments are still necessary to provide a clearer definition of the structures that traps the Pb atoms in order to prevent the formation of metallic NPs as observed in the non aged samples. Nevertheless, the consequence of this behavior is to allow the development of an atomic redistribution process that leads to the exclusive formation of bidimensional NP array at the silica–silicon interface.

V. CONCLUSIONS

In summary, we studied the formation of NPs in silica films implanted with Pb atoms. In contrast to usual ion beam synthesis behavior, the formation of large Pb NPs inside the silica film can be avoided when the implanted samples are submitted to an aging process followed by high temperature FA treatment. In this case, the Pb atoms redistribute, leaving the silica film with a rather pristine aspect, and form a dense bidimensional array of epitaxial NPs presenting small size dispersion and short range order. This behavior indicates that, during the aging process, the Pb atoms became trapped in the silica matrix within rather small and thermally stable structures that only dissociate at high temperatures. Their thermal stability seems to be a more general property of elements or compounds that can develop structures presenting rather low interface free energy with the surrounding silica matrix.

ACKNOWLEDGMENTS

The authors acknowledge the support from the founding agencies CAPES and CNPq. The use of the infrastructure of CME-UFRGS is also acknowledged.

[1] W. Skorupa, L. Rebohle, and T. Gebel, Appl. Phys. A: Mater. Sci. Process. **76**, 1049 (2003).
[2] J. M. J. Lopes, F. C. Zawislak, M. Behar, P. F. P. Fichtner, L. Rebohle, and W. Skopura, J. Appl. Phys. **94**, 6059 (2003).
[3] H.-J. Fitting, Opt. Mater. (Amsterdam, Neth.) **31**, 1891 (2009).
[4] A. Nakajima, T. Futatsugi, H. Nakao, T. Usuki, N. Horiguchi, and N. Yokoyama, J. Appl. Phys. **84**, 1316 (1998).
[5] P. Dimitrakis, E. Kapetanakis, D. Tsoukalas, D. Skarlatos, C. Bonafos, G. Bem Asssayag, A. Claverie, M. Perego, M. Fanciulli, V. Soncini, R. Sotgiu, A. Agarwal, M. Ameen, C. Sohl, and P. Normand, Solid-State Electron. **48**, 1511 (2004).
[6] T. W. Ko, J. C. Kim, H. C. Choi, K.-H. Park, S. H. Lee, K.-M. Kim, W.-R. Lee, and G. D. Lee, Appl. Phys. Lett. **91**, 053506 (2007).
[7] G. De Marchi, G. Mattei, P. Mazzoldi, C. Sada, and A. Miotello, J. Appl. Phys. **92**, 4249 (2002).
[8] K. H. Heinig, T. Müller, B. Schmidt, M. Strobel, and W. Möller, Appl. Phys. A: Mater. Sci. Process. **77**, 17 (2003).
[9] A. Meldrum, R. Lopez, R. H. Magruder, L. A. Boatner, and C. W. White, in *Topics in Applied Physics*, edited by H. Bernas (Springer-Verlag, Berlin, 2010), Vol. 116, p. 255.
[10] F. Ren, X. H. Xiao, G. X. Cai, J. B. Wang, and C. Z. Jiang, Appl. Phys. A: Mater. Sci. Process. **96**, 317 (2009).
[11] F. Kremer, J. M. J. Lopes, F. C. Zawislak, and P. F. P. Fictner, Appl. Phys. Lett. **91**, 083102 (2007).
[12] P. Letellier, A. Mayaffre, and M. Turmine, Phys. Rev. B **76**, 045428 (2007).
[13] Q. S. Mei and K. Lu, Prog. Mater. Sci. **52**, 1175 (2007).
[14] A. Safaei, M. Attarian Shandiz, S. Sanjabi, and Z. H. Barber, J. Phys. Chem. C **112**, 99 (2008).
[15] M. Bernardi, A. Sgarlata, M. Fanfoni, A. Balzarotti, and N. Motta, Appl. Phys. Lett. **93**, 031917 (2008).
[16] P. Patnaik, *Handbook of Inorganic Chemicals* (McGraw-Hill, New York, 2002).
[17] J. Gavarri, J. Solid State Chem. **23**, 327 (1978).
[18] C. Rajesh, C. Majumder, M. G. R. Rajan, and S. K. Kulshreshtha, Phys. Rev. B **72**, 235411 (2005).
[19] A. A. Shvartsburg and M. F. Jarrold, Chem. Phys. Lett. **317**, 615 (2000).
[20] R. Pushpa, U. Waghmare, and S. Narasimhan, Phys. Rev. B **77**, 045427 (2008).
[21] H. H. Farrell and C. D. Van Siclen, J. Vac. Sci. Technol. B **25**, 1441 (2007).